Title	The role of carbonate and sulfite additives in propylene carbonate-based electrolytes on the formation of SEI layers at graphitic Li-ion battery anodes
Authors	Bhatt, Mahesh Datt;O'Dwyer, Colm
Publication date	2014-06-21
Original Citation	Bhatt, M. D. and O'Dwyer, C. (2014) 'The Role of Carbonate and Sulfite Additives in Propylene Carbonate-Based Electrolytes on the Formation of SEI Layers at Graphitic Li-Ion Battery Anodes', Journal of The Electrochemical Society, 161(9), pp. A1415-A1421. doi: 10.1149/2.0931409jes
Type of publication	Article (peer-reviewed)
Link to publisher's version	http://jes.ecsdl.org/content/161/9/A1415.full.pdf+html - 10.1149/2.0931409jes
Rights	© The Author(s) 2014. Published by ECS. This is an open access article distributed under the terms of the Creative Commons Attribution Non-Commercial No Derivatives 4.0 License (CC BY-NC-ND, http://creativecommons.org/licenses/by-nc-nd/4.0/), which permits non-commercial reuse, distribution, and reproduction in any medium, provided the original work is not changed in any way and is properly cited. For permission for commercial reuse, please email: oa@electrochem.org. [DOI: 10.1149/2.0931409jes] All rights reserved. - http://creativecommons.org/licenses/by-nc-nd/4.0/
Download date	2024-04-16 09:32:50
Item downloaded from	https://hdl.handle.net/10468/6107

The Role of Carbonate and Sulfite Additives in Propylene Carbonate-Based Electrolytes on the Formation of SEI Layers at Graphitic Li-Ion Battery Anodes

Mahesh Datt Bhatt and Colm O'Dwyer*,z

Department of Chemistry, University College Cork, Cork, Ireland
Tyndall National Institute, Lee Maltings, Cork, Ireland

Density functional theory (DFT) was used to investigate the effect of electrolyte additives such as vinylene carbonate (VC), vinyl ethylene carbonate (VEC), vinyl ethylene sulfite (VES), and ethylene sulfite (ES) in propylene carbonate (PC)-based Li-ion battery electrolytes on SEI formation at graphitic anodes. The higher desolvation energy of PC limits Li$^+$ intercalation into graphite compared to solvated Li$^+$ in EC. Li$^+$(PC)$_3$ clusters are found to be unstable with graphite intercalation compounds and become structurally deformed, preventing decomposition mechanisms and associated SEI formation in favor of co-intercalation that leads to exfoliation. DFT calculations demonstrate that the reduction decomposition of PC and electrolyte additives is such that the first electron reduction energies scale as ES > VES > VEC > PC. The second electron reduction follows ES > VES > VEC > VC > PC. The reactivity of the additives under consideration follows ES > VES > VEC > VC. The data demonstrate the supportive role of certain additives, particularly sulfites, in PC-based electrolytes for SEI film formation and stable cycling at graphitic carbon-based Li-ion battery anodes without exfoliation or degradation of the anode structure.

The lithium ion battery has been one of the primary power sources driving the digital age, and witnessed a resurgence in interest with the advent of nanoscale materials and advances in cell performance.[1–6] Much of the processes and mechanisms underpinning carbonate-based electrolytes in Li-ion batteries, particularly at the anode, still need to be resolved.[7,8]

Some commonly used organic solvents are ethylene carbonate (EC), propylene carbonate (PC), dimethyl carbonate (DMC), diethyl carbonate (DEC), and ethyl methyl carbonate (EMC) etc. These organic electrolytes are decomposed during intercalation of lithium ions into graphite anode, resulting in the formation of the crucial solid electrolyte interphase (SEI) film.[9–11] This film plays an important role in determining capacity retention, cycle life and safety concerns in lithium ion batteries.[12,13] SEI films typically comprise Li$_2$O, Li$_2$CO$_3$ and related carbonates, LiF (depending on salt used), and polymer phases together with olefins.[14] Effective SEI films provide stable surface passivation without significant reduction in electron conduction (higher transfer resistance). On carbon (graphite) anodes, stable SEI films are crucial for stable cycling and are formed below ∼0.8 V vs. Li$^+$/Li.

In practical applications of lithium-ion batteries, the selection of the electrode material is critical, particularly when using high surface area nanomaterials.[15] Enhanced chemical stability against electrolyte oxidation and reduction, high ionic conductivity, high boiling points, and low melting points are required, as well as the ability to solvate a wide range of lithium salts such as LiPF$_6$, LiBF$_4$ or LiClO$_4$,[16–21] in aprotic and organic solvents such as ethylene carbonate (EC), propylene carbonate (PC), their mixtures, and ionic liquids. The decomposition mechanism of organic solvent and subsequent formation of SEI films near the graphite anode is a major research topic in lithium ion batteries from theoretical[22–30] and experimental[31–39] standpoints, and one of the least understood.

These electrolytes have proven to be the most efficient in terms of cyclability.[40] An EC electrolyte has higher dielectric constant and lower viscosity than a PC-based electrolyte, a thus a superior solvent. These properties favor salt dissociation and high ionic diffusion rates, resulting in improved ionic conductivity. Due to lower melting point (36.2°C) of EC, it is a solid at room temperature. Therefore, mixtures of EC with liquid solvents such as a PC and linear carbonates such as an ethyl methyl carbonate (EMC) are useful in practical applications.[41–43]

It is well known that a lithium-ion battery with a graphite anode and an electrolyte EC can be cycled, while the charging of a similar battery in an electrolyte PC gives rise to exfoliation of graphite.[44–47] Balbuena and co-workers performed theoretical calculations on the reductive decomposition intermediates of EC and PC in absence of graphite to determine the difference in the interaction of Li$^+$ ions with EC and PC.[36,38] PC is less suitable for a graphitic anode due to its tendency to co-intercalate into graphite during the first charge process which leads to the destruction via exfoliation of the graphite structure.[27,48–50] Therefore, many methods have been developed to solve this problem. One effective method is the use of film-forming electrolyte additives which are reduced predominantly on the graphite anode surface during the first charging process. These additives mainly consist of two functional groups namely such as vinylene compounds and sulfites. The VC molecule is a reactive additive that reacts on the anode surface. Previous spectroscopic studies showed that VC forms polyalkyl Li-carbonate species after its polymerization on a lithiated graphite surface.[51] Such species suppress both solvent and salt anion reduction. Han and Lee investigated possible reaction products and the thermodynamic stability of Li$^+$-EC and Li$^+$-VC by nucleophilic addition reaction with CH$_3$O$^-$.[33] Similarly, other additives such as vinyl ethylene carbonate (VEC), ethylene sulfite (ES), and vinyl ethylene sulfite (VES) also play an important role in the protection of the structure of the graphitic anode from exfoliation/destruction by PC, and have been used to enhance anode stability in modern nanomaterial-based anodes.[52,53]

Aurbach et al.[54] proposed the two-electron reduction mechanism of EC based on the component analysis of SEI films as shown in Fig. 1, which has been confirmed in some specific density functional theory (DFT)-based ab initio molecular dynamics simulations.[55]

Here, we first investigate the electronic structures of ternary graphite intercalation compounds (GICs), Li$^+$(S)$_{n=1-4}$C$_{14}$ (S = EC, PC) using density functional theory to determine the best choice of a range of carbonate and sulfite additives for PC-based electrolytes that promote stable SEI film formation at a graphite anode in Li-ion batteries. Quantum chemical computations give accurate energies of reactions and intermediates, including decomposition mechanisms that are key to SEI formation and stability in cycling for Li-ion batteries.[56] The data described here detail the thermodynamically favorable mechanisms and

*Electrochemical Society Active Member.
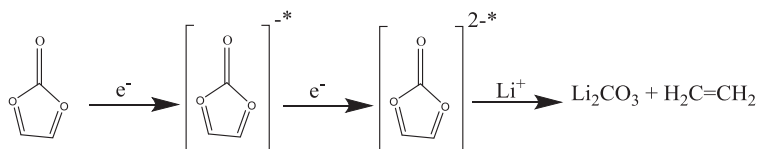zE-mail: c.odwyer@ucc.ie

Figure 1. Schematic diagram of two electron reduction mechanism of ethylene carbonate to linear carbonates.

limitations of PC electrolytes on stable SEI formation at graphitic electrodes.

We also present an investigation into the electronic structures of various forms of additives such as vinylene carbonate (VC), vinyl ethylene carbonate (VEC), vinyl ethylene sulfite (VES), and ethylene sulfite (ES) in propylene carbonate (PC)-based electrolyte solutions and from computations, compare their relative effectiveness at preventing the exfoliation of the graphite anode over Li insertion and SEI formation. Calculations confirm VEC, VES, and ES additives are superior to VC for PC-based electrolytes and consistent with the associated first and second electron reduction energies. The calculated theoretical results and findings may aid the choice of electrolyte additives in experimental battery systems that use layered graphitic materials in carbonate electrolytes.

Computational Details

An isolated PC solvent and electrolyte additive (VC, VEC, ES, VES) molecule and their clusters including a lithium ion are optimized by using the B3LYP/6-31G (d) parameter in the liquid phase. The solvent effect is included in both optimization and single point calculations through the polarized continuum using the conductor polarizable continuum model (CPCM)[57–61] with tetrahydrofuran (THF) dielectric. Density functional theory calculations are performed with hybrid parameter B3LYP as implemented in Gaussian 09W.[62] The hybrid parameter B3LYP consists of exchange correlation function generalized gradient approximation (GGA) in the Becke,[63] Lee-Yang-Parr,[64] and VWN formula 5.[65] The basis set is chosen as 6-31G (d) for our calculations. The approximate basis set superposition error (BSSE)[66] for all clusters is calculated using Counter Poise (CP) method and is observed to be negligibly small. The first electron reduction energy ($E_1 = E_{11} + E_{12}$) and the second electron reduction energy (E_2) for PC and additives are calculated according to the reduction schemes in Fig. 2 using EC as an example.
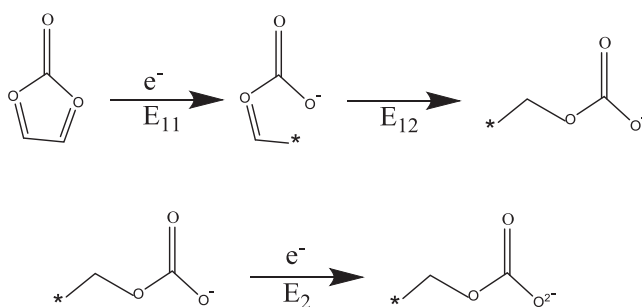

Figure 2. The first electron reduction energy ($E_1 = E_{11} + E_{12}$) and the second electron reduction energy (E_2) for EC.

The calculated optimized structures of propylene carbonate (PC), vinylene carbonate (VC), vinyl ethylene carbonate (VEC), vinyl ethylene sulfite (VES), ethylene sulfite (ES) including their open carbonate anions are shown in Figs. 3a and 3b respectively.

The optimized structures of the lithiated clusters $Li^+(PC)_3(A)$ [A = VC, VEC, VES, and ES] complexes are shown in Fig. 4.

Results and Discussion

We first examine the solvation structures of the lithium ion in both EC and PC. Figure 5 shows the optimized structures for $Li^+(S)_{n=1-4}$ [S = EC, PC] using DFT calculations. From Fig. 5, it is clear that all solvation structures other than $Li^+(EC)_4$ maintain planar structures and $Li^+(EC)_4$ maintains a quasi-tetrahedron. Such structural transitions from the pyramidal configuration to a planar one defines the final state of Li^+ ion intercalation into graphite, and influenced by the asymmetric nature of PC.
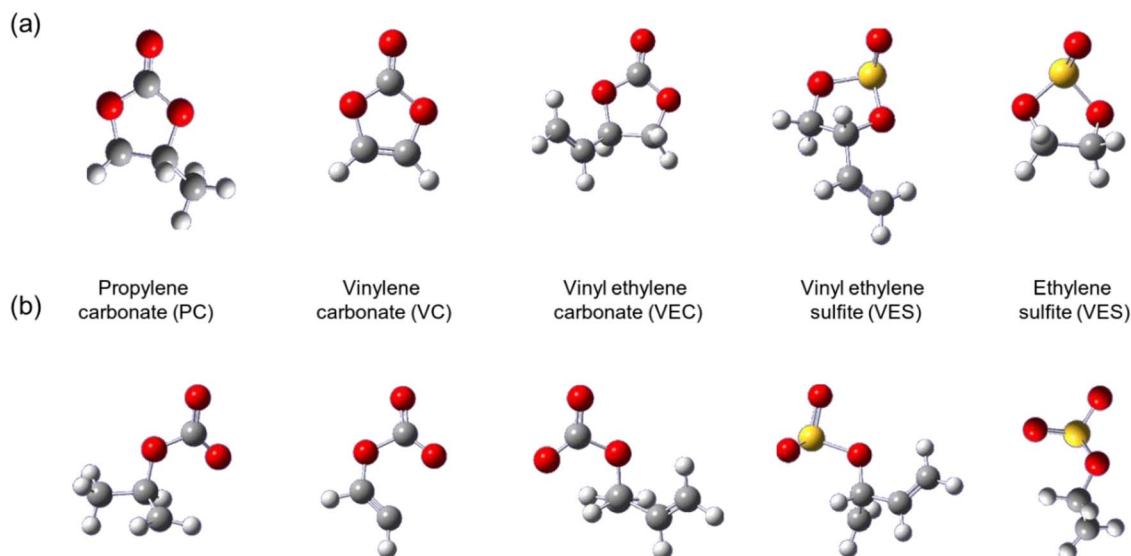

Figure 3. Optimized structures of propylene carbonate (PC), vinylene carbonate (VC), vinyl ethylene carbonate (VEC), vinyl ethylene sulfite (VES), ethylene sulfite (ES) including their open carbonate anions. Red atoms are oxygen, yellow atoms are sulfur, gray atoms are carbon, and white atoms are hydrogen.
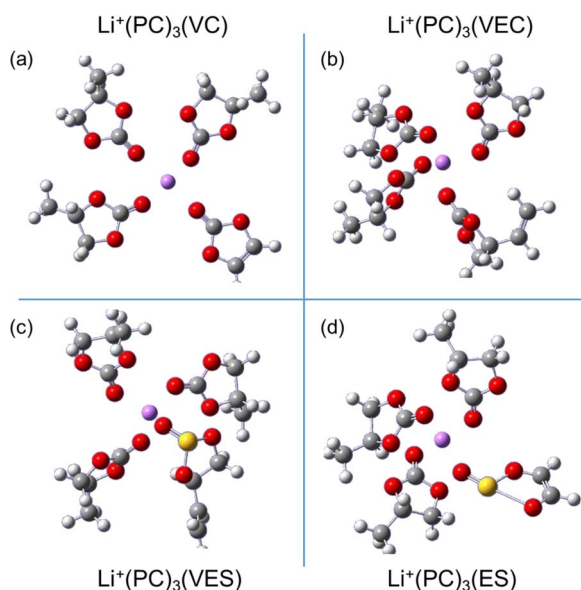
Figure 4. Optimized structures of Li$^+$(PC)$_3$(A) [A = (a) VC, (b) VEC, (c) VES, and (d) ES] complexes.

Using the optimized structures in Fig. 5, the solvation and desolvation energies are calculated as follows:

$$\Delta E_{solv} = E_{total}[Li^+(S)_{n=1-4}] - E_{total}[Li^+] - n E_{total}[S] \quad [1]$$

where $E_{total}[Li^+(S)_{n=1-4}]$, $E_{total}[Li^+]$, and $E_{total}[S]$ represent the total free energy for Li$^+$(S)$_{n=1-4}$ (S = EC, PC), Li$^+$, and S, respectively.

$$\Delta E_{desolv} = E_{total}[Li(S)_{n=1-4}] + E_{total}[S] - E_{total}[Li(S)_{n+1}] \quad [2]$$

where $E_{total}[Li(S)_{n=1-4}]$, $E_{total}[S]$, and $E_{total}[Li(S)_{n+1}]$ represent the total free energy for Li$^+$(S)$_{n=1-4}$ (S = EC, PC), Li$^+$, and S respectively.

These calculated solvation and desolvation energies are shown in Table I and Table II, respectively.

Table I. Solvation energy (kcal/mol) for Li$^+$(S)$_{n=1-4}$ (S = EC, PC) in the liquid phase at the level of B3LYP/6-31G (d).

Solvation number	Li$^+$(EC)$_{n=1-4}$ (kcal/mol)	Li$^+$(PC)$_{n=1-4}$ (kcal/mol)
n = 1	−13.84	−13.43
n = 2	−26.97	−26.68
n = 3	−37.65	−36.93
n = 4	−47.72	−46.88

Table II. Desolvation energy (kcal/mol) for Li$^+$(S)$_{n=1-4}$ (S = EC, PC) in the liquid phase at the level of B3LYP/6-31G (d).

Solvation number	Li$^+$(EC)$_{n=1-4}$ (kcal/mol)	Li$^+$(PC)$_{n=1-4}$ (kcal/mol)
n = 1	13.12	14.15
n = 2	9.62	11.25
n = 3	6.45	9.55

It is clear from Table I that the solvation energy of Li$^+$-EC complex is greater than the Li$^+$-PC complex, which demonstrates the stability of EC compared to PC due to strong binding of Li$^+$ to EC molecules compared to PC molecules. The solvation energy is also found to decrease with increase in solvation number for both EC and PC.

From Table II, PC gives rise to a higher desolvation energy compared to EC, which suggests that Li$^+$ may have more difficulty intercalating into the anode from PC-based solvents. To examine this effect, we consider the oxidation of the electrolyte by examining the highest occupied molecular orbital (HOMO) of EC and PC from calculations. The HOMO energy of EC and PC are calculated to be −8.19 and −8.13 eV, respectively as shown in Table III, indicating that the oxidative decomposition activity is in the order PC > EC. On this basis, EC is more stable against oxidation than PC. However, due to the higher dielectric constant of EC, Li$^+$ coordinates more easily with EC than with PC. The lowest unoccupied molecular orbital (LUMO) energies of EC and PC are 0.86 and 0.87 eV, respectively, indicating the reductive decomposition activity follows EC > PC; EC is thus stable against reduction. The calculated solvation energy and desolvation energy of Li$^+$ for EC and PC are found consistent with literature data.[67,68]
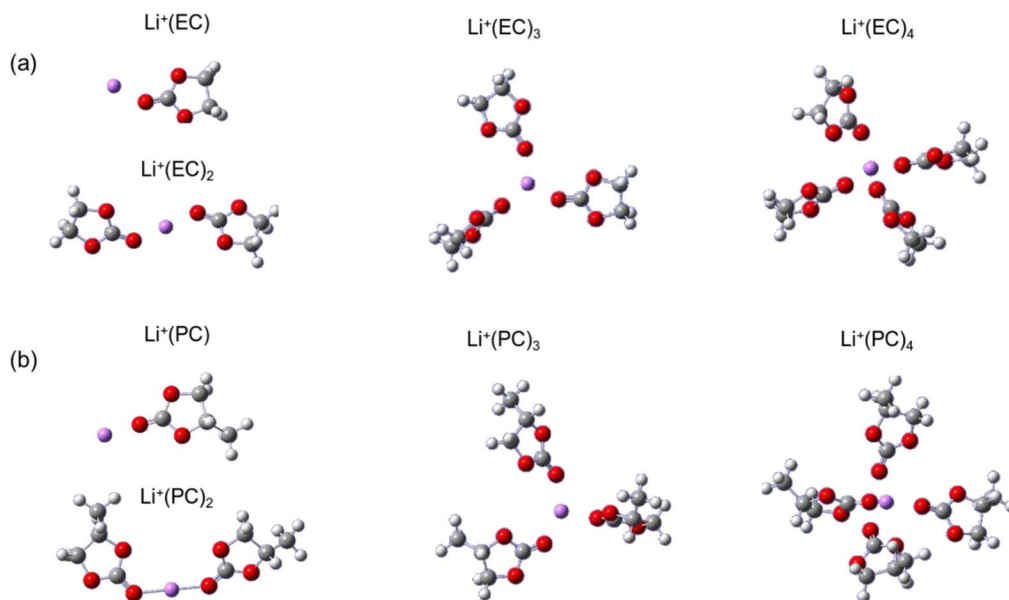

Figure 5. Solvation structures of Li$^+$(S)$_{n=1-4}$ [S = (a) EC and (b) PC] complexes. The purple atom is lithium.

Table III. Total energy E_T (in Hartree) and frontier molecular orbital energy (in eV) of solvents (EC and PC) and additives (VC, VEC, VES, and ES) at the level of B3LYP/6-31G (d).

| Solvent/ Additives	E_T	E_{HOMO}	E_{LUMO}	Dielectric constants
EC	−342	−8.19	0.86	90.50 (at 40 °C)
PC	−381.84703	−8.13	0.87	65.50 (at 25 °C)
VC	−341.27954	−7.32	−0.36	...
VEC	−419.93109	−7.75	−0.54	...
VES	−779.95654	−7.36	−0.69	...
ES	−702.53876	−6.55	−1.19	...

The energetics of solvents (EC, PC) and additives (A = VC, VEC, VES, ES) as well as the first and second electron reduction energies of solvent (PC) and its additives (A = VC, VEC, VES, ES) were determined. The corresponding total energy and frontier molecular orbital energies of additives (A = VC, VEC, VES, ES) and propylene carbonate (PC) were provided in Table III. From Table III, we observe that the energy level of the LUMO of any additive A is much lower than that of PC solvent itself. Based upon molecular orbital theory, a molecule with lower LUMO energy should be a better acceptor and more reactive on the negatively charged surface of the anode. In this sense, additive A will be reduced prior to the PC solvent during the first charge process. The reactivity of additives based on the LUMO energy is found in the order ES > VES > VEC > VC. This is likely be due to the stability of –SO$_3$ group as compared to –CO$_3$ group. The calculated frontier orbital energies of solvents and additives other than ES are consistent with related DFT calculations.[69,70] In the presence of ES, any SEI film formed during charging are considered to be more soluble to solvated Li$^+$(ES)$_n$, than to Li$^+$(PC)$_n$ moieties. Additionally, comparison of these findings to voltammetric investigations in experimental work using similar solvents, suggests that while PC does not in itself help to form SEI that prevent co-intercalation and thus graphite exfoliation, ES can potentially initiate reduction processes in PC leading to more effective SEI film formation at the graphite surface. A lithium-ion cell using a graphitic anode can be cycled with good coulometric efficiency using PC:DMC that maintains a degree of solvation of PC below 2, i.e. Li$^+$(PC)$_{n < 2}$.[71,73]

With calculations for the optimized lithated solvent complexes, the energetics of ternary graphite intercalation compounds (GICs), Li$^+$(S)$_{n = 1-4}$ (S = EC, PC) can be examined as a model system replicating a graphite anode in the presence of EC and PC electrolytes. The ternary GIC energy is calculated according to:

$$\Delta E[Li^+ (S)_{n=1-4} C_{14}]$$
$$= E_{total}[Li^+ (S)_{n=1-4} C_{14}] + n E_{total}[S] - E[C_{14}] \quad [3]$$

where $E_{total}[Li^+ (S)_{n=1-4} C_{14}]$, $E_{total}[S]$, and $E[C_{14}]$ represent the total free energy of a ternary GIC, a solvent (EC or PC) molecule, and graphite, respectively.

Table IV lists the energetics of Li$^+$(S)$_{n = 1-4}$C$_{14}$ (S = EC, PC). Our DFT calculations show that Li$^+$(EC)$_{n = 1-4}$C$_{14}$ are all more stable than Li$^+$(PC)$_{n = 1-3}$C$_{14}$ for the same solvation number. The energetics of Li$^+$(PC)$_{n = 4}$C$_{14}$ are not necessary to determine since Li$^+$(PC)$_{n = 3}$C$_{14}$ is found already to be unstable (positive energy). The ternary GICs for both EC and PC become less stable as the
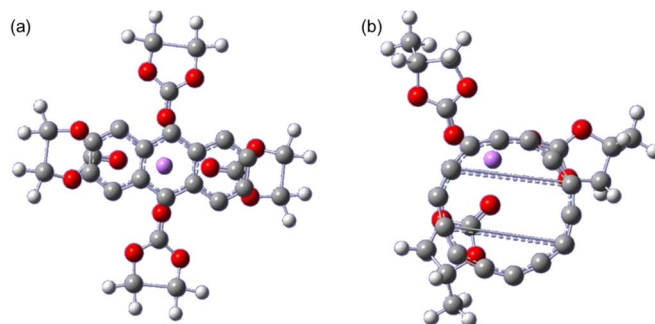
Figure 6. Structures of (a) Li$^+$(EC)$_{n = 4}$C$_{14}$ and (b) Li$^+$(PC)$_{n = 3}$C$_{14}$.

number of solvent molecules increases due to the steric repulsions between the ternary GIC and graphene layer. It is of particular interest to observe that Li$^+$(PC)$_{n = 3}$C$_{14}$ is energetically unfavorable. On other hand, Li$^+$(EC)$_{n = 1-4}$C$_{14}$ energies all are negative and thermodynamically stable. Zhao et al.[72] performed similar calculations on Li$_x$(THF) (x = 2–8) intercalated in graphite using a GGA-PBE functional, but no intercalation energy was reported however.

The calculated structures of Li$^+$(EC)$_{n = 4}$C$_{14}$ and Li$^+$(PC)$_{n = 3}$C$_{14}$ are shown in Fig. 6. It is clear from Fig. 6 that no exfoliation in graphite occurs for Li$^+$(EC)$_{n = 4}$C$_{14}$. However, exfoliation occurs for Li$^+$(PC)$_{n = 3}$C$_{14}$. PC was determined earlier to be unstable compared to EC and Li$^+$(PC)$_3$C$_{14}$ complex is found to be unstable for a stable ternary GIC to be formed, limiting the possibility of coherent SEI film formation at the graphite anode. These findings indicate the necessity of choice electrolyte additives to enhance the reduction of PC to promote SEI film formation; no such problem exists for EC to even higher degrees of solvation. The solvation of Li$^+$ in PC can be altered by the use of higher temperatures (abnormal operating conditions)[73] or by using a different solvent. Theoretical examination of the effective of a range of additives (A = VC, VEC, VES, or ES) to PC solvents to facilitate the two step reduction to form stable SEI films on Li-ion graphitic anodes is considered next.

Table V lists the first and second electron reduction energies of PC and additives. The first electron reduction energy (E_1) of PC and additive in solution is found in the order PC > VC. However, we find from calculations that A > PC for A = VEC, VES, and ES. If the process is limited electrochemically to the first electron reduction for PC-based electrolyte for example, then additives other than VC are effective in promoting SEI film formation near the graphite anode. The second electron reduction energy (E_2) is A > PC (Table V). Here, all additives including VC have lower values of E_2 than PC, and are likely to undergo second electron reduction to produce Li$_2$CO$_3$ with additives VC and VEC, and Li$_2$SO$_3$ with VES and ES, found in most SEI films. In some experimental measurements using differential electrochemical mass spectrometry, Li$_2$S and Li$_2$O are also capable of being formed, but at potentials (vs Li$^+$/Li) greater than (i.e. preceding) PC decomposition.[67] In case of PC alone, it may be decomposed before undergoing second electron reduction due to high value of E_2. The calculated values are significant in determining and explaining the

Table IV. The energy (kcal/mol) of Li$^+$(S)$_{n = 1-4}$C$_{14}$ (S = EC, PC) at the level of B3LYP/6-31G (d).

System	Li$^+$(EC)$_{n = 1-4}$C$_{14}$ (kcal/mol)	Li$^+$(PC)$_{n = 1-4}$C$_{14}$ (kcal/mol)
n = 1	−226.88	−177.13
n = 2	−148.32	−69.67
n = 3	−84.65	77.94
n = 4	−27.53	...

Table V. The calculated first electron reduction energies, E_1 and second electron reduction energies, E_2 (in eV) of PC and additives (VC, VEC, VES, and ES) at the level of B3LYP/6-31G (d).

Solvent/Additives	E_1 (eV)	E_2 (eV)
PC	−2.66	−2.16
VC	−2.40	−3.67
VEC	−2.88	−4.22
VES	−3.72	−4.25
ES	−3.85	−4.34

Table VI. The calculated characteristics of PC with and without additives (VC, VEC, VES, and ES) at the level of B3LYP/6-31G (d).
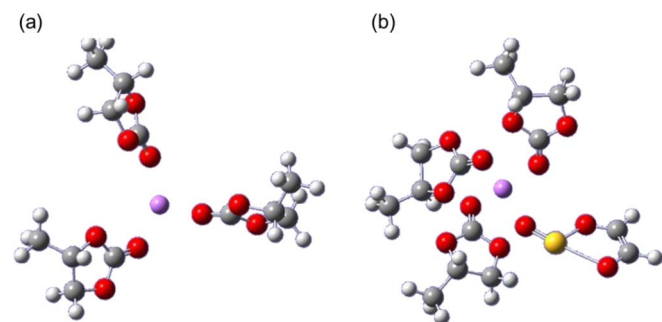
Complexes	Minimum C=O distance (Å)	Minimum C-O distance (Å)	Minimum Li$^+$-O distance (Å)	Charge on Li$^+$ (e)	ΔG (kcal/mol)	ΔH (kcal/mol)
Li$^+$(PC)$_3$	1.218	1.331	1.941	0.51	−9.69	−15.20
Li$^+$(PC)$_3$-VC	1.211	1.387	1.974	0.45	−60.58	−27.26
Li$^+$(PC)$_3$-VEC	1.217	1.333	1.956	0.35	−73.37	−36.63
Li$^+$(PC)$_3$-VES	1.216	1.332	1.947	0.34	−76.72	−42.83
Li$^+$(PC)$_3$-ES	1.211	1.332	1.950	0.35	−115.32	−98.17

comparative effectiveness for SEI film formation at layered graphitic anodes.

Next, we present calculations for the characteristics and structure of PC with and without additives for Li$^+$(PC)$_3$ and Li$^+$(PC)$_3$A complexes (A = VC, VEC, VES, ES) considered as model complexes at the limit of solvation prior to exfoliation (reduction to linear carbonates and SEI film formation). The corresponding characteristics are given in Table VI. As reported in Table VI, the change in Gibb's free energies and enthalpy are found in the order ES > VES > VEC > VC, consistent with the observed order of their respective LUMO energies. The minimum C=O bond length calculated for PC decreases by 0.001–0.006 Å, while C-O bong length increases by 0.001–0.056 Å when additives are used. The minimum Li$^+$-O distance in PC is found to increase by a maximum of 0.033 Å when VC is used. The optimized structures of Li$^+$(PC)$_3$ and Li$^+$(PC)$_3$ES complexes are shown in Fig. 7.

Finally, the theoretical IR spectra of PC with and without additives as Li$^+$(PC)$_{n=1-3}$A complexes (A = VC, VEC, VES, ES) are calculated and analyzed comparatively. The IR spectra of Li$^+$(PC)$_3$A complex (A = VC, VEC, VES, ES), together with isolated PC and each of the additive molecules, are shown in Figs. 8a and 8b respectively.

From Fig. 8, it is clear that the C=O frequency of PC increases in the order ES > VES > VEC > VC, while the C-O frequency of PC decreases in the same order with additives consistent with the change in their respective bond lengths due to these interactions. Some new vibrations from the complexes are found at low frequencies (400–1000 cm^{-1}) due to the presence of additives, which demonstrates the influence of additives on the decomposition of PC prior to SEI film formation near graphite anode. Moreover, the IR spectra of PC with all additives (that includes the increasing fraction of PC) are reproduced in Fig. 9. From these IR spectra, it is important to notice that there is decrease in C=O and C-O frequency with increase in content of PC compared to VC. We also observe an increase in C=O and C-O frequencies with a greater PC content compared to VEC, VES, and ES. This theoretical IR examination will allow comparison to experiment and aid in identifying the vibronic structure of optimized electrolyte-additive complexes in electrolytes.

Characteristically, the C=O frequency is found to be 1818.30, 1804.02, and 1799.26 cm^{-1} for PC:VC ratios of 1:1, 2:1, and 3:1 respectively, while the corresponding values for PC:VEC contents are found to be 1799.26, 1804.02, and 1813.54 cm^{-1}. The specific alteration to vibrational response demonstrates that VEC, VES, and ES additives are superior to VC for PC-based electrolytes and consistent with the associated first and second electron reduction energy calculations.

Figure 7. Optimized structures of (a) Li$^+$(PC)$_3$ and (b) Li$^+$(PC)$_3$ES complexes.
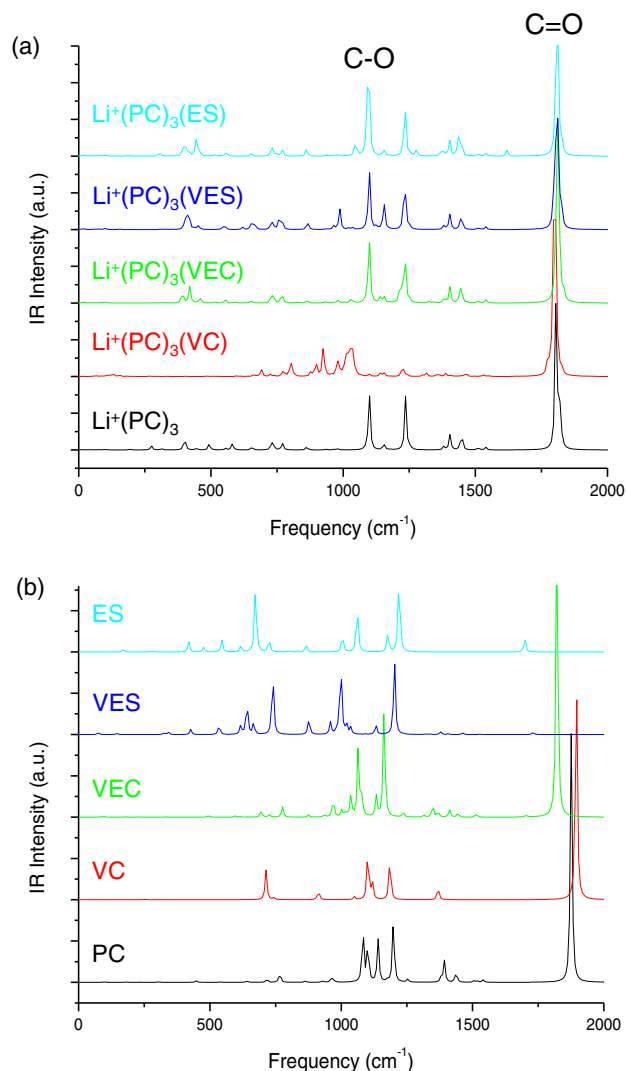
Figure 8. IR spectra of Li$^+$(PC)$_3$A complexes (A = VC, VEC, VES, ES) and isolated PC and additive molecules.
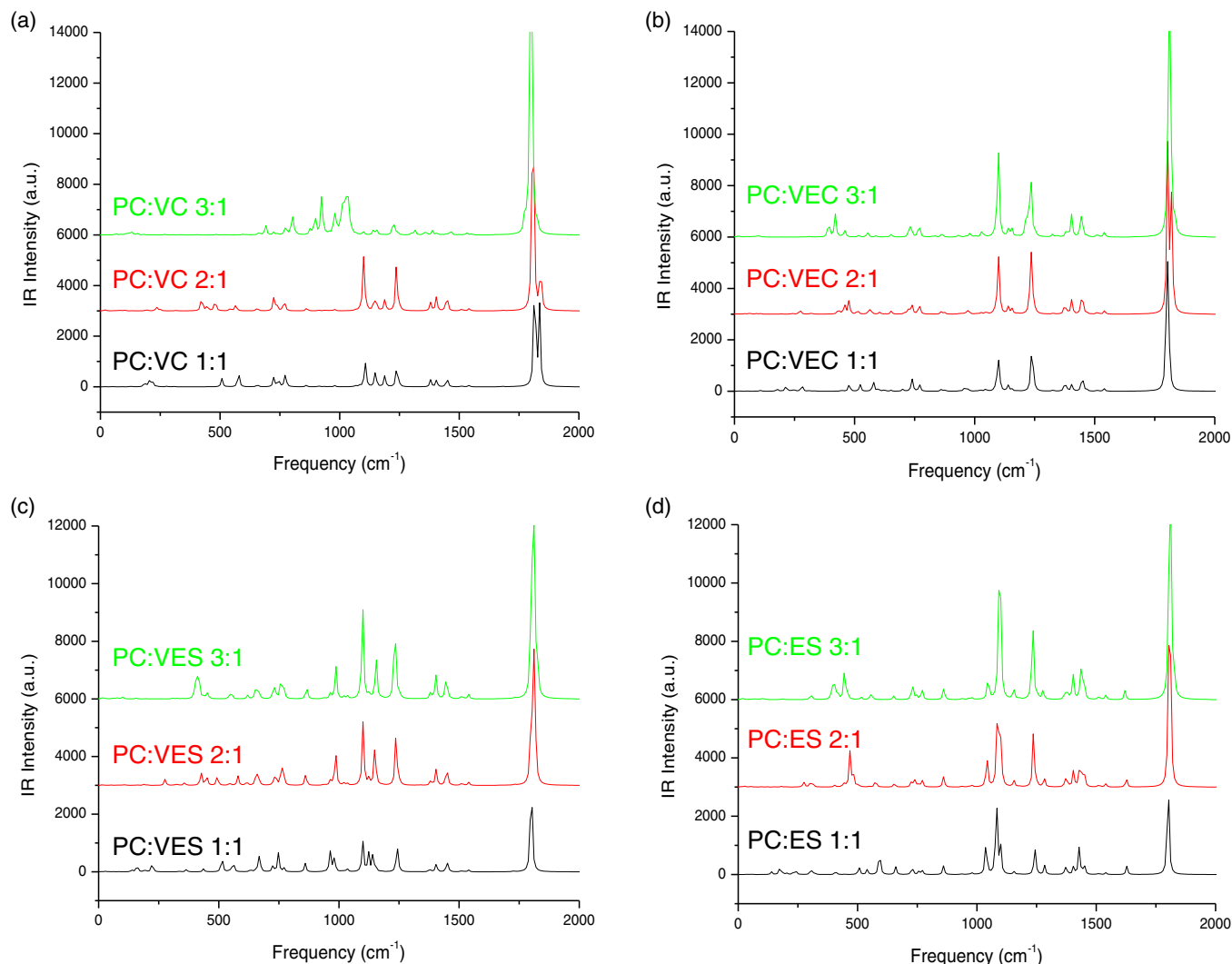
Figure 9. IR spectra of PC as a function of the PC:additive ratio for additives (a) VC, (b) VEC, (c) VES, and (d) ES.

Conclusions

Density functional theory methods were used to investigate the effect of electrolyte additives such as vinylene carbonate (VC), vinyl ethylene carbonate (VEC), vinyl ethylene sulfite (VES), and ethylene sulfite (ES) in propylene carbonate (PC)-based Li-ion battery electrolytes in the liquid phase at the level of B3LYP/6-31G (d) using the polarizable continuum model in a tetra hydrofuran (THF) dielectric. The higher desolvation energy of PC limits Li$^+$ intercalation into graphite compared to solvated Li$^+$ in EC. The higher HOMO and LUMO energies of EC confirms a lesser degree of oxidative and reductive decomposition for PC. The interaction energies of Li$^+$ in PC and EC with respect to a graphite intercalation compound demonstrates limited SEI formation near the graphite anode for PC-based electrolyte complexes due to a preference for exfoliation by co-intercalation. Li$^+$(PC)$_3$ clusters are found to be unstable with GIC's and become structurally deformed, preventing decomposition mechanisms and associated SEI formation in favor of co-intercalation.

Calculations demonstrate that the reduction decomposition of PC and electrolyte additives is such that the first electron reduction in solution is found in the order PC > VC, and scales as ES > VES > VEC >PC. Importantly, PC cannot be decomposed with VC as an additive during the first electron reduction. The second electron reduction follows ES > VES > VEC > VC > PC, which clearly indicates the decomposition of PC after second electron reduction to form the SEI film near the graphite anode. The reactivity

of the additives under consideration is found as ES > VES > VEC > VC. Theoretical IR vibrational characteristics of PC with and without additives also indicate the bonding within solvated complexes. The data demonstrate the supportive role of certain additives, particularly sulfites, in PC-based electrolytes for SEI film formation and stable cycling at graphitic carbon-based Li-ion battery anodes without exfoliation or degradation of the anode structure.

References

1. J. B. Goodenough and Y. Kim, *Chemistry of Materials*, **22**, 587 (2009).
2. B. Scrosati and J. Garche, *Journal of Power Sources*, **195**, 2419 (2010).
3. M. J. Armstrong, C. O'Dwyer, W. J. Macklin, and J. D. Holmes, *Nano Research*, **7**, 1 (2014).
4. C. K. Chan, H. Peng, G. Liu, K. McIlwrath, X. F. Zhang, R. A. Huggins, and Y. Cui, *Nature nanotechnology*, **3**, 31 (2008).
5. M. Osiak, H. Geaney, E. Armstrong, and C. O'Dwyer, *Journal of Materials Chemistry A*, **2014**, 9433 (2014).

6. P. Poizot, S. Laruelle, S. Grugeon, L. Dupont, and J. Tarascon, *Nature*, **407**, 496 (2000).
7. J. B. Goodenough and K. S. Park, *Journal of the American Chemical Society*, **135**, 1167 (2013).
8. J. B. Goodenough, *Accounts of chemical research*, **46**, 1053 (2013).
9. M. Armand and J.-M. Tarascon, *Nature*, **451**, 652 (2008).
10. J.-M. Tarascon and M. Armand, *Nature*, **414**, 359 (2001).
11. M. S. Whittingham, *Chemical Reviews*, **104**, 4271 (2004).
12. L. Lu, X. Han, J. Li, J. Hua, and M. Ouyang, *Journal of power sources*, **226**, 272 (2013).
13. G. Pistoia, *Lithium batteries: new materials, developments, and perspectives*, Elsevier Science Ltd (1994).
14. J. O. Besenhard, M. Winter, J. Yang, and W. Biberacher, *Journal of Power Sources*, **54**, 228 (1995).
15. B. A. Korgel, *The Journal of Physical Chemistry Letters*, **5**, 749 (2014).
16. Y. Abu-Lebdeh and I. Davidson, *Journal of The Electrochemical Society*, **156**, A60 (2009).
17. Y. Abu-Lebdeh and I. Davidson, *Journal of Power Sources*, **189**, 576 (2009).
18. H. Duncan, N. Salem, and Y. Abu-Lebdeh, *Journal of The Electrochemical Society*, **160**, A838 (2013).
19. P. Isken, C. Dippel, R. Schmitz, R. Schmitz, M. Kunze, S. Passerini, M. Winter, and A. Lex-Balducci, *Electrochimica Acta*, **56**, 7530 (2011).
20. D. Moosbauer, S. Zugmann, M. Amereller, and H. J. Gores, *Journal of Chemical & Engineering Data*, **55**, 1794 (2010).
21. K. Xu and A. von Cresce, *Journal of Materials Chemistry*, **21**, 9849 (2011).
22. P. Arora, R. E. White, and M. Doyle, *Journal of the Electrochemical Society*, **145**, 3647 (1998).
23. D. Aurbach, *Journal of Power Sources*, **89**, 206 (2000).
24. D. Aurbach, Y. Ein-Eli, O. Chusid, Y. Carmeli, M. Babai, and H. Yamin, *Journal of The Electrochemical Society*, **141**, 603 (1994).
25. D. Aurbach, Y. Ein-Ely, and A. Zaban, *Journal of The Electrochemical Society*, **141**, L1 (1994).
26. D. Aurbach, M. D. Levi, E. Levi, and A. Schechter, *The Journal of Physical Chemistry B*, **101**, 2195 (1997).
27. D. Aurbach, B. Markovsky, I. Weissman, E. Levi, and Y. Ein-Eli, *Electrochimica acta*, **45**, 67 (1999).
28. E. Peled, D. Golodnitsky, C. Menachem, and D. Bar-Tow, *Journal of the Electrochemical Society*, **145**, 3482 (1998).
29. A. Schechter, D. Aurbach, and H. Cohen, *Langmuir*, **15**, 3334 (1999).
30. Z. Shu, R. McMillan, and J. Murray, *Journal of The Electrochemical Society*, **140**, 922 (1993).
31. E. Endo, M. Ata, K. Tanaka, and K. Sekai, *Journal of The Electrochemical Society*, **145**, 3757 (1998).
32. E. Endo, K. Tanaka, and K. Sekai, *Journal of The Electrochemical Society*, **147**, 4029 (2000).
33. Y.-K. Han, S. U. Lee, J.-H. Ok, J.-J. Cho, and H.-J. Kim, *Chemical physics letters*, **360**, 359 (2002).
34. T. Li and P. B. Balbuena, *Chemical Physics Letters*, **317**, 421 (2000).
35. A. Márquez and P. B. Balbuena, *Journal of The Electrochemical Society*, **148**, A624 (2001).
36. Y. Wang and P. B. Balbuena, *The Journal of Physical Chemistry B*, **106**, 4486 (2002).
37. Y. Wang and P. B. Balbuena, *The Journal of Physical Chemistry A*, **106**, 9582 (2002).
38. Y. Wang, S. Nakamura, K. Tasaki, and P. B. Balbuena, *Journal of the American Chemical Society*, **124**, 4408 (2002).
39. Y. Wang, S. Nakamura, M. Ue, and P. B. Balbuena, *Journal of the American Chemical Society*, **123**, 11708 (2001).
40. D. Aurbach, Y. Gofer, M. Ben-Zion, and P. Aped, *Journal of Electroanalytical Chemistry*, **339**, 451 (1992).
41. B. Klassen, R. Aroca, M. Nazri, and G. Nazri, *The Journal of Physical Chemistry B*, **102**, 4795 (1998).
42. S.-i. Tobishima and A. Yamaji, *Electrochimica Acta*, **28**, 1067 (1983).
43. S.-I. Tobishima, J.-I. Yamaki, and T. Okada, *Electrochimica acta*, **29**, 1471 (1984).
44. J. Besenhard and H. Fritz, *Journal of Electroanalytical Chemistry and Interfacial Electrochemistry*, **53**, 329 (1974).
45. M. Chhowalla, H. S. Shin, G. Eda, L.-J. Li, K. P. Loh, and H. Zhang, *Nature chemistry*, **5**, 263 (2013).
46. Y. Hernandez, V. Nicolosi, M. Lotya, F. M. Blighe, Z. Sun, S. De, I. T. McGovern, B. Holland, M. Byrne, Y. K. Gun'Ko, J. J. Boland, P. Niraj, G. Duesberg, S. Krishnamurthy, R. Goodhue, J. Hutchison, V. Scardaci, A. C. Ferrari, and J. N. Coleman, *Nature Nanotechnology*, **3**, 563 (2008).
47. V. Nicolosi, M. Chhowalla, M. G. Kanatzidis, M. S. Strano, and J. N. Coleman, *Science*, **340**, 1420 (2013).
48. M. Fujimoto, Y. Shoji, Y. Kida, R. Ohshita, T. Nohma, and K. Nishio, *Journal of power sources*, **72**, 226 (1998).
49. H. Kaneko, K. Sekine, and T. Takamura, *Journal of power sources*, **146**, 142 (2005).
50. H.-L. Zhang, C.-H. Sun, F. Li, C. Liu, J. Tan, and H.-M. Cheng, *The Journal of Physical Chemistry C*, **111**, 4740 (2007).
51. D. Aurbach, K. Gamolsky, B. Markovsky, Y. Gofer, M. Schmidt, and U. Heider, *Electrochimica Acta*, **47**, 1423 (2002).
52. T. D. Bogart, A. M. Chockla, and B. A. Korgel, *Current Opinion in Chemical Engineering*, **2**, 286 (2013).
53. T. Kennedy, E. Mullane, H. Geaney, M. Osiak, C. O'Dwyer, and K. M. Ryan, *Nano letters* (2014).
54. D. Aurbach, M. Daroux, P. Faguy, and E. Yeager, *Journal of The Electrochemical Society*, **134**, 1611 (1987).
55. K. Leung and J. L. Budzien, *Physical Chemistry Chemical Physics*, **12**, 6583 (2010).
56. K. Leung, Y. Qi, K. R. Zavadil, Y. S. Jung, A. C. Dillon, A. S. Cavanagh, S. H. Lee, and S. M. George, *J. Am. Chem. Soc.*, **133**, 14741 (2011).
57. M.-H. Baik, T. Ziegler, and C. K. Schauer, *Journal of the American Chemical Society*, **122**, 9143 (2000).
58. V. Barone and M. Cossi, *The Journal of Physical Chemistry A*, **102**, 1995 (1998).
59. J. R. Keeffe, S. Gronert, M. E. Colvin, and N. L. Tran, *Journal of the American Chemical Society*, **125**, 11730 (2003).
60. I. Krossing, A. Bihlmeier, I. Raabe, and N. Trapp, *Angewandte Chemie International Edition*, **42**, 1531 (2003).
61. A. J. Sillanpää, R. Aksela, and K. Laasonen, *Physical chemistry chemical physics*, **5**, 3382 (2003).
62. M. Frisch, G. Trucks, H. Schlegel, G. Scuseria, M. Robb, J. Cheeseman, G. Scalmani, V. Barone, B. Mennucci, G. Petersson, H. Nakatsuji, M. Caricato, X. Li, H. P. Hratchian, A. F. Izmaylov, J. Bloino, G. Zheng, J. L. Sonnenberg, M. Hada, M. Ehara, K. Toyota, R. Fukuda, J. Hasegawa, M. Ishida, T. Nakajima, Y. Honda, O. Kitao, H. Nakai, T. Vreven, J. J. A. Montgomery, J. E. Peralta, F. Ogliaro, M. Bearpark, J. J. Heyd, E. Brothers, K. N. Kudin, V. N. Staroverov, R. Kobayashi, J. Normand, K. Raghavachari, A. Rendell, J. C. Burant, S. S. Iyengar, J. Tomasi, M. Cossi, N. Rega, J. M. Millam, M. Klene, J. E. Knox, J. B. Cross, V. Bakken, C. Adamo, J. Jaramillo, R. Gomperts, R. E. Stratmann, O. Yazyev, A. J. Austin, R. Cammi, C. Pomelli, J. W. Ochterski, R. L. Martin, K. Morokuma, V. G. Zakrzewski, G. A. Voth, P. Salvador, J. J. Dannenberg, S. Dapprich, A. D. Daniels, O. Farkas, J. B. Foresman, J. V. Ortiz, J. Cioslowski, and D. J. Fox, *Gaussian 09, Revision A. 1. Wallingford CT: Gaussian* (2009).
63. A. D. Becke, *Physical Review A*, **38**, 3098 (1988).
64. C. Lee, W. Yang, and R. Parr, *Phys. Rev. A*, **38**, 3098 (1988).
65. S. H. Vosko, L. Wilk, and M. Nusair, *Canadian Journal of Physics*, **58**, 1200 (1980).
66. S. F. Boys and F. d. Bernardi, *Molecular Physics*, **19**, 553 (1970).
67. M. D. Bhatt, M. Cho, and K. Cho, *Journal of Solid State Electrochemistry*, **16**, 435 (2012).
68. K. Tasaki, A. Goldberg, J.-J. Liang, and M. Winter, *ECS Transactions*, **33**, 59 (2011).
69. S.-D. Xu, Q.-C. Zhuang, J. Wang, Y.-Q. Xu, and Y.-B. Zhu, *Int. J. Electrochem. Sci*, **8**, 8058 (2013).
70. W. Yao, Z. Zhang, J. Gao, J. Li, J. Xu, Z. Wang, and Y. Yang, *Energy & Environmental Science*, **2**, 1102 (2009).
71. Y. Yamada, Y. Koyama, T. Abe, and Z. Ogumi, *The Journal of Physical Chemistry C*, **113**, 8948 (2009).
72. Y. Zhao, Y.-H. Kim, L. J. Simpson, A. C. Dillon, S.-H. Wei, and M. J. Heben, *Physical Review B*, **78**, 144102 (2008).
73. H. Xiang, C. Chen, J. Zhang, and K. Amine, *Journal of Power Sources*, **195**, 604 (2010).